ELSEVIER

European Journal of Pharmacology 416 (2001) 11–18

ejp

www.elsevier.nl/locate/ejphar

Phenol derivatives accelerate inactivation kinetics in one inactivation-deficient mutant human skeletal muscle Na^+ channel

Gertrud Haeseler [a,*], Alf Piepenbrink [a], Johannes Bufler [b], Reinhard Dengler [b], Hartmut Hecker [c], Jeffrey Aronson [d], Siegfried Piepenbrock [a], Martin Leuwer [e]

[a] *Department of Anaesthesia, OE 8050 Hannover Medical School, D-30623 Hannover, Germany*
[b] *Department of Neurology and Neurophysiology, OE 8050 Hannover Medical School, D-30623 Hannover, Germany*
[c] *Department of Biometrics, OE 8050 Hannover Medical School, D-30623 Hannover, Germany*
[d] *Department of Clinical Pharmacology, The University of Oxford, Oxford, UK*
[e] *University Department of Anaesthesia, The University of Liverpool, Liverpool, UK*

Received 9 November 2000; received in revised form 31 January 2001; accepted 16 February 2001

Abstract

Altered inactivation kinetics in skeletal muscle Na^+ channels due to mutations in the encoding gene are causal for the alterations in muscle excitability in nondystrophic myotonia. Na^+ channel blockers like lidocaine and mexiletine, suggested for therapy of myotonia, do not reconstitute inactivation in channels with defective inactivation in vitro. We examined the effects of four methylated and/or halogenated phenol derivatives on one heterologously expressed inactivation-deficient Paramyotonia congenita-mutant (R1448H) muscle Na^+ channel in vitro. All these compounds accelerated delayed inactivation of R1448H-whole-cell currents during a depolarization and delayed accelerated recovery from inactivation. The potency of these effects paralleled the potency of the drugs to block the peak current amplitude. We conclude that the investigated phenol derivatives affect inactivation-deficient Na^+ channels more specifically than lidocaine and mexiletine. However, for all compounds, the effect on inactivation was accompanied by a substantial block of the peak current amplitude.

Keywords: Phenol derivative; Channel inactivation; Skeletal muscle

1. Introduction

Voltage-sensitive Na^+ channels are membrane proteins essential for the generation and propagation of action potentials in excitable tissues. Alterations in Na^+ channel gating might have important consequences in vivo. For the skeletal muscle Na^+ channel, such consequences are exemplified by a group of hereditary muscle diseases, including Paramyotonia congenita, in which hyperexcitability of the sarcolemma is attributed to the expression of mutant Na^+ channels with altered inactivation phenotypes (Lehmann-Horn and Rüdel, 1995). Although the mutations identified so far in affected patients occurred in different regions of the Na^+ channel protein, the alterations in channel gating shown by heterologously expressed mutant channels were surprisingly uniform (Yang et al., 1994). Almost all mutant channels studied to date have impaired inactivation (Hoffman et al., 1995). Additional findings were altered voltage-dependence of inactivation and accelerated recovery from inactivation (Chahine et al., 1994b; Hoffman et al., 1995; Lehmann-Horn and Rüdel, 1995; Yang et al., 1994). Na^+ channel blockers, such as lidocaine or mexiletine, suggested for long- or short-term therapy of myotonia (Lehmann-Horn and Rüdel, 1995), turned out to be unable to reconstitute inactivation in Na^+ channels with defective inactivation (Hudson et al., 1995; Sah et al., 1998). In contrast, the phenol derivative 3-methyl-4-chlorophenol (4-chloro-*m*-cresol), used as a bacteriostatic stabilizer in some pharmaceutical formulations, is an effective blocker of normal and mutant muscle Na^+ channels, and, in addition, restores channel dysfunction to

* Corresponding author. Tel.: +49-511-532-2070; fax: +49-511-532-5649.
E-mail address: Haeseler.Gertrud@MH-Hannover.de (G. Haeseler).

0014-2999/01/$ - see front matter
PII: S0014-2999(01)00857-3

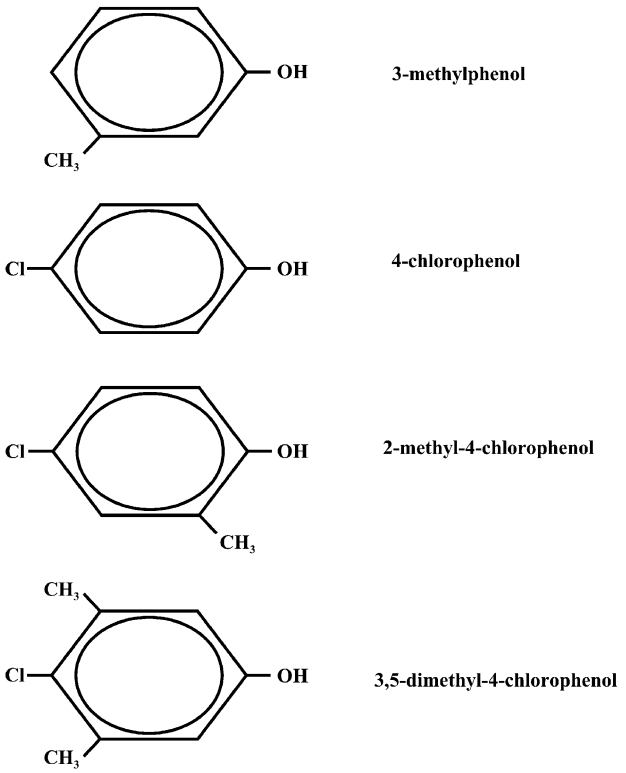

Fig. 1. Structures of the phenol derivatives 3,5-dimethyl-4-chlorophenol, 2-methyl-4-chlorophenol, 4-chlorophenol, 2-methylphenol.

normal in a Paramyotonia congenita mutant in vitro (Haeseler et al., 1999).

Consequently, the aim of this study was to characterize the effects of four different methylated and/or halogenated phenol derivatives (see Fig. 1) on one representative inactivation-deficient skeletal muscle Na^+ channel, the Paramyotonia congenita mutant R1448H. R1448H exchanges extracellular positioned arginine for histidine in the S4 segment of domain 4 in the α-subunit of skeletal muscle voltage-gated Na^+ channels.

2. Methods

2.1. Molecular biology

Methods have been described in more detail previously (Haeseler et al., 1999). In brief, R1448H mutant α-subunits of human muscle Na^+ channels were heterologously expressed in human embryonic kidney (HEK 293) cells. Transfected cells were a gift from Prof. Lehmann-Horn, Ulm, Germany. Permanent expression was achieved by selection for resistance to the aminoglycoside antibiotic geneticin G418 (Life Technology, Eggenstein, Germany) (Mitrovic et al., 1994). Successful channel expression was verified electrophysiologically, confirming the results previously obtained for that clone in several investigations (Chahine et al., 1994b; Haeseler et al., 1999; Yang et al., 1994).

2.2. Solutions

3,5-Dimethyl-4-chlorophenol (Sigma, Deisenhofen, Germany) was prepared as a 1 M stock solution in methanol, and 2-methyl-4-chlorophenol (Fluka Chemicals, Deisenhofen, Germany), 4-chlorophenol (Fluka Chemicals), and 3-methylphenol (Sigma) were dissolved directly in the bath solution immediately before the experiments. The bath solution contained (mM) NaCl 140, $MgCl_2$ 1.0, KCl 4.0, $CaCl_2$ 2.0, HEPES 5.0, dextrose 5.0. Patch electrodes contained (mM) $CsCl_2$ 130, $MgCl_2$ 2.0, EGTA 5.0, HEPES 10. The amount of methanol corresponding to the test concentration of 3,5-dimethyl-4-chlorophenol was added to the control solution.

2.3. Experimental set-up

Standard whole-cell voltage-clamp experiments (Hamill et al., 1981) were performed at 20°C. Each experiment consisted of test recordings with the drug present at only one concentration, and of drug-free control recordings before and after the test. Eight cells were exposed to bath solution only instead of test solution in order to assess spontaneous, time-dependent changes in voltage-dependence of inactivation and time-dependent kinetics of inactivation and recovery from fast inactivation.

2.4. Current recordings and analysis

For data acquisition and further analysis we used the EPC9 digitally controlled amplifier in combination with Pulse and Pulse Fit software (HEKA Electronics, Lambrecht, Germany). The EPC9 provides automatic subtraction of capacitive and leakage currents by means of a prepulse (P/-4) protocol. The data were filtered at 10 kHz and digitized at 20 μs per point. Input resistance of the patch pipettes was at 1.8–2.5 MΩ, cell capacitances ranged from 9 to 15 pF; residual series resistance (after 50% compensation) was 1.2–2.5 MΩ. All test experiments were performed within 5 min of patch rupture. Under these experimental conditions, time-dependent voltage shifts of steady-state availability plots in control conditions were less than −2 mV (Haeseler et al., 2000). Voltage-activated currents were studied by applying different voltage-clamp protocols described in Results or in the appropriate figure legends.

2.5. Statistics

All the data are presented descriptively as means ± S.D. Statistical analysis of the concentration–response plots was performed in order to reveal possible differences in potency with respect to the pulse protocol applied. Curve

fitting and parameter estimation of the Hill plots was performed using the program "Non-linear Least Squares Regression" of S-PLUS (S-PLUS 2000 Professional Release 1, Copyright © 1988–1999 MathSoft, Cambridge MA) yielding estimates for IC_{50} and n_H with their standard error (S.E.). The differences between the parameter values (IC_{50} and n_H) of two independent data sets were entered into the common model as shift parameters ΔIC_{50} and Δn_H activated for all data of the second data set. The corresponding (asymptotic) *t*-value was used to test the null hypothesis of no parameter difference. The null hypothesis was rejected when the p value was less than 0.05.

3. Results

3.1. Block of resting channels

In all, 101 cells were included in the study. Average Na^+ inward currents in the control experiments following depolarization from −100 to 0 mV were 4.2 ± 1.8 nA.

Maximum inward currents elicited by 10-ms pulses going from either hyperpolarized membrane potentials (−150 and −100 mV), or a membrane potential close to the physiological resting potential (−70 mV, Hodgkin and Horowicz, 1959) to 0 mV were reversibly suppressed by all compounds (see Fig. 2). Residual currents in the pres-

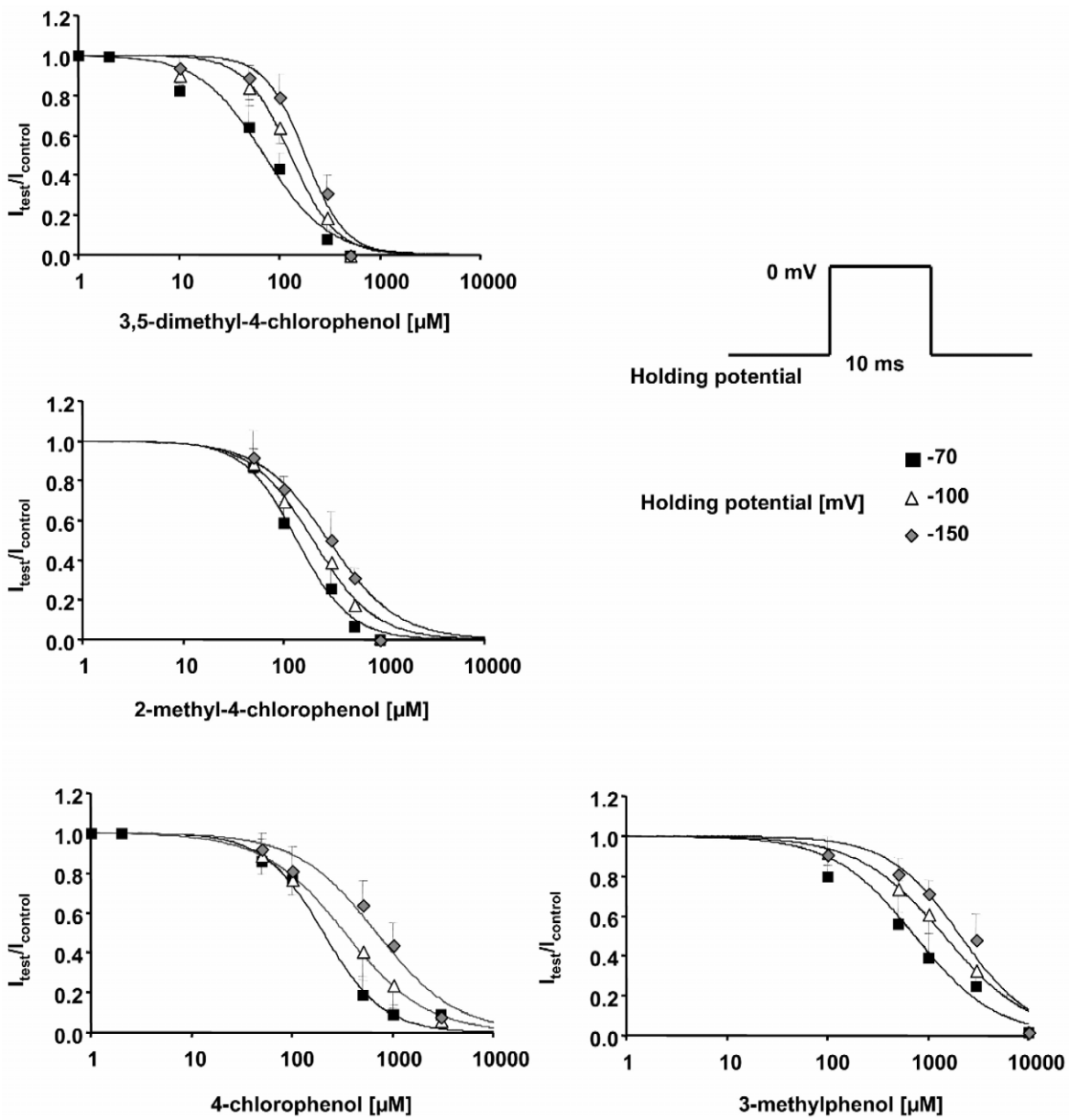

Fig. 2. Concentration-dependent reduction in test pulse current with respect to control ($I_{test}/I_{control}$, mean ± S.D.) induced by the different phenol compounds. The data were derived from at least six different experiments at each concentration tested. Depolarizing pulses to 0 mV (10-ms duration) were started from −150, −100, or −70 mV. Solid lines are Hill fits to the data. The potency of all drugs was significantly increased at holding potentials of −100 and −70 mV, compared to −150 mV.

ence of drug, derived from at least six different experiments for each drug concentration, were plotted against the applied concentration. Hill fits ($I_{Na^+_{test}}/I_{Na^+_{control}} = [1 + ([C]/IC_{50})^{n_H}]^{-1}$) to the concentration–response plots yielded the concentration for half-maximum channel blockade (IC_{50}) and the Hill coefficient n_H. IC_{50} values for block of resting channels at −150 mV were 183 ± 11 μM (3,5-dimethyl-4-chlorophenol), 302 ± 14 μM (2-methyl-4-chlorophenol), 732 ± 58 μM (4-chlorophenol), and 2280 ± 195 μM (3-methylphenol). The respective Hill coefficient estimates were 1.4 ± 0.1, 1.6 ± 0.2, 1.1 ± 0.1 and 1.1 ± 0.1. As depicted in Fig. 2, the potency of all compounds to block the peak inward currents was significantly increased at more depolarized holding potentials (−100 and −70 mV), relative to −150 mV. At −70 mV, the IC_{50} values were reduced about threefold with respect to the values obtained at −150 mV for all compounds, suggesting a higher affinity for inactivated channels.

3.2. Affinity for the fast-inactivated state estimated by steady-state availability shifts

The affinity of the drugs for the inactivated state was further assessed applying a double-pulse protocol. Families of 50-ms inactivating prepulses to varying prepulse potentials (from −150 to −5 mV) induced a steady-state of inactivated (control) or inactivated-blocked (test) channels at a given prepulse potential, reducing the amplitude of the subsequent test pulse. Boltzmann fits to the resulting relative current–prepulse voltage plots yielded the prepulse potential at half-maximum channel availability $V_{0.5}$, which determines the position of the curve along the voltage axis, and the slope factor k ($I/I_{max} = (1 + \exp((V_{test} - V_{0.5})/k))^{-1}$). In control conditions, the position of the steady-state availability curve along the voltage axis reflects the apportionment of rested and fast-inactivated channels at a given membrane potential. Summarized control data for R1448H ($n = 71$) showed that half of the channels were unavailable at −69 ± 5.6 mV, owing to fast inactivation. The slope factor k was 12.1 ± 0.6. In the presence of drug, the amount of block achieved increased with consecutive membrane depolarization, relative to the block achieved at −150 mV prepulse potential. This increase in blocking potency in the voltage range of channel inactivation was revealed by a drug-induced negative shift of the availability curve (see Fig. 3), which showed concentration dependence. Control experiments obtained from five cells that were exposed to bath solution instead of test solution revealed that time-dependent negative shifts during 3 min of whole-cell recording were negligible (−1.1 ± 0.6 mV). To estimate the dissociation constant K_d for each compound from the fast-inactivated state of the channel, we employed a model developed by Bean et al. (1983) for the example of lidocaine effects on Purkinje fibers. The model is based on the assumption that the higher amount of channel block achieved with consecutive membrane depolarization, revealed by the drug-induced hyperpolarizing shift, reflects the apportionment of channels between resting and fast-inactivated states as well as the higher binding affinity for the inactivated state with respect to the resting state. This model offers the advantage of having been used frequently in the past to estimate inactivated affinity for Na^+ channel blockers (Fan et al., 1996). However, one caveat is that the reduction of the voltage drop through the remaining uncompensated series resistance, which is proportional to the ion current block achieved by the respective compound, tends to underestimate the effect of higher drug concentrations ($> IC_{50}$ for rest block) by approximately 5 mV. The concentration-dependence of the shift in the midpoints was fitted to the equation $\Delta V_{0.5} = k\ln[1/(1 + [C]/K_d)]$ where $\Delta V_{0.5}$ is the shift in the midpoint in each concentration of each compound tested (mean, $n > 4$), k the slope factor for the availability curve derived from Boltzmann fits to the current–voltage plots, [C] the applied concentration, and K_d the dissociation constant from the inactivated state (see Fig. 3B). As resting state binding was neglected for that fit, the model can only be regarded as an approximation, which tends to underestimate the affinities for the inactivated with respect to the resting state. Estimates for K_d derived from that fit were 38 ± 7 μM (3,5-dimethyl-4-chlorophenol), 57 ± 10 μM (2-methyl-4-chlorophenol), 126 ± 15 μM (4-chlorophenol), and 543 ± 125 μM (3-methylphenol).

3.3. Acceleration of the Na^+ current decay phase by phenol derivatives

The time course of Na^+ channel inactivation was assessed during a 40-ms depolarization from −100 to 0 mV. Time constants of channel inactivation τ_h were obtained by fitting a biexponential curve to the decay of currents: ($I(t) = a_0 + a_1\exp(-t/\tau_{h1}) + a_2\exp(-t/\tau_{h2})$).

In control conditions prior to drug administration, τ_{h1} was 1.6 ± 0.3 ms. The amplitude of the second, slow component τ_{h2} of 5.3 ± 1.5 ms made up 23 ± 13% (n = 93). All phenol derivatives accelerated the decay of whole-cell currents. For all compounds, however, this effect was apparent only at concentrations at which there was substantial block of the peak current amplitude. Values obtained for τ_{h1} in the presence of drug were: 1.2 ± 0.3 and 1.0 ± 0.1 ms in 100 and 300 μM 3,5-dimethyl-4-chlorophenol, 1.3 ± 0.3, 1.0 ± 0.3, and 0.8 ± 0.08 ms in 100, 300 and 500 μM 2-methyl-4-chlorophenol, 1.1 ± 0.2 and 0.7 ± 0.2 ms in 500 and 1000 μM 4-chlorophenol, and 1.5 ± 0.5 and 0.6 ± 0.1 ms in 1000 and 3000 μM 3-methylphenol. The amplitude of the second slow component was reduced accordingly in higher drug concentrations to 7 ± 3% in 100 μM 3,5-dimethyl-4-chlorophenol, 2.7 ± 1.5% in 300 μM 2-methyl-4-chlorophenol, 3.6 ± 2.8% in 1000 μM 4-chlorophenol and 3 ± 3% in 3000 μM 3-methylphenol.

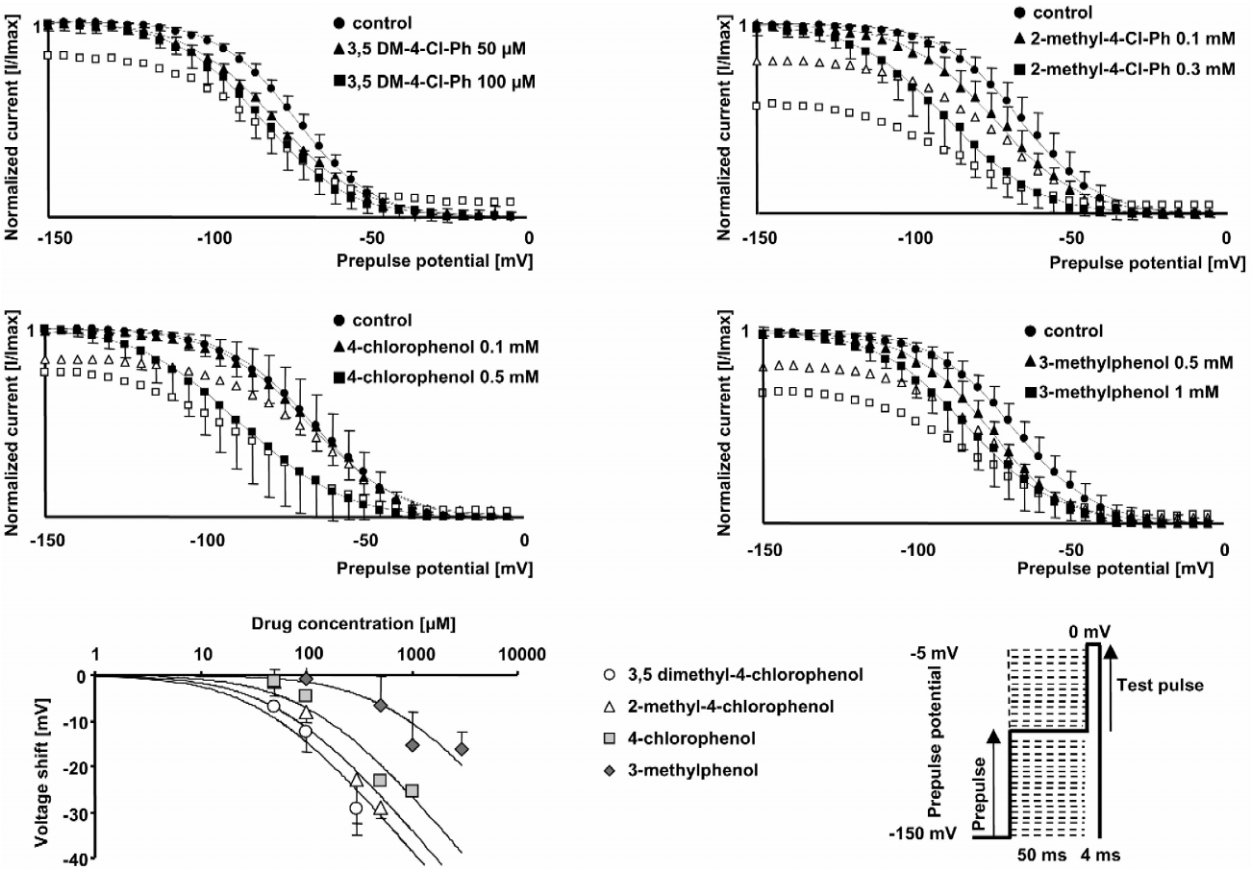

Fig. 3. Interference of phenol derivatives with fast-inactivated channels, assessed by shifts in the steady-state availability curve. (A–D) Steady-state availability curves assessed by a two-pulse protocol in control conditions (circles) and in the presence of representative concentrations of each compound (triangles and/or squares). Each symbol represents the mean fractional current ($n > 4$ for each concentration and each clone) elicited by a 4-ms test pulse to 0 mV, after a 50-ms inactivating prepulse from −150 mV to the indicated prepulse potential. Currents were normalized to maximum values (in each series at −150 mV prepotential); solid lines represent the best Boltzmann fit [$I/I_{max} = (1 + \exp((V_{test} - V_{0.5})/k))^{-1}$] to the data. Error bars are standard deviations. In the presence of drug, currents were normalized either to maximum values in the presence of drug (filled symbols) or to maximum values in control conditions (empty symbols). All compounds shifted the midpoints of the curves in the direction of more negative prepulse potentials, reflecting an additional reduction in channel availability at depolarized prepotentials (compared with the block achieved at −150 mV). For 50 µM 3,5-dimethyl-4-chlorophenol, the peak current suppression at −150 mV was minimal. The empty triangles were therefore omitted for the sake of clarity. (E) Concentration-dependence of negative voltage shifts of the midpoints ($\Delta V_{0.5}$ [mV], mean ± S.D.) of the steady-state availability plots relative to the starting values for all drugs examined. Solid lines are least-squares fits to the equation $\Delta V_{0.5} = k\ln[(1/(1 + [C]/K_d)]$, yielding the dissociation constant K_d from the inactivated state for each compound.

Five control experiments were performed on cells that were exposed to bath solution instead of test solution in the same time interval after seal formation. No spontaneous changes in time-dependent inactivation were observed. The starting values for τ_{h1} were 1.84 ± 0.3 ms, after 3 min of whole-cell recording, τ_{h1} was 1.83 ± 0.36 ms. The amplitude of the slow component (6.4 ± 1.8 and 5.6 ± 2 ms) remained at 16 ± 8%.

3.4. Effects of phenol derivatives on recovery from fast inactivation

The time of membrane repolarization required to remove fast inactivation was assessed at −100 mV by a double-pulse protocol with varying time intervals (up to 100 ms) between the inactivating prepulse and the test pulse (Fig. 4). The time constants of recovery, τ_{rec}, were derived from monoexponential or biexponential fits to the fractional current after recovery from inactivation, plotted against the time interval between the inactivating prepulse and the test pulse: ($I(t) = a_0 + a_1\exp(-t/\tau_{rec1}) + a_2\exp(-t/\tau_{rec2})$). Without drug, the data fitted well to a monoexponential, yielding a time constant, τ_{rec1}, of 1.8 ± 0.6 ms ($n = 45$). In the presence of all compounds, the fit contained a second, slow component of recovery, τ_{rec2}, of 30 ± 18 ms (3,5-dimethyl-4-chlorophenol), 33 ± 20 ms (2-methyl-4-chlorophenol), 30 ± 15 ms (4-chlorophenol), and 28 ± 12 ms (3-methylphenol), which made up 14–18% of the current amplitude in concentrations close to the IC_{50} for rest block. The fast component, τ_{rec1}, was minimally

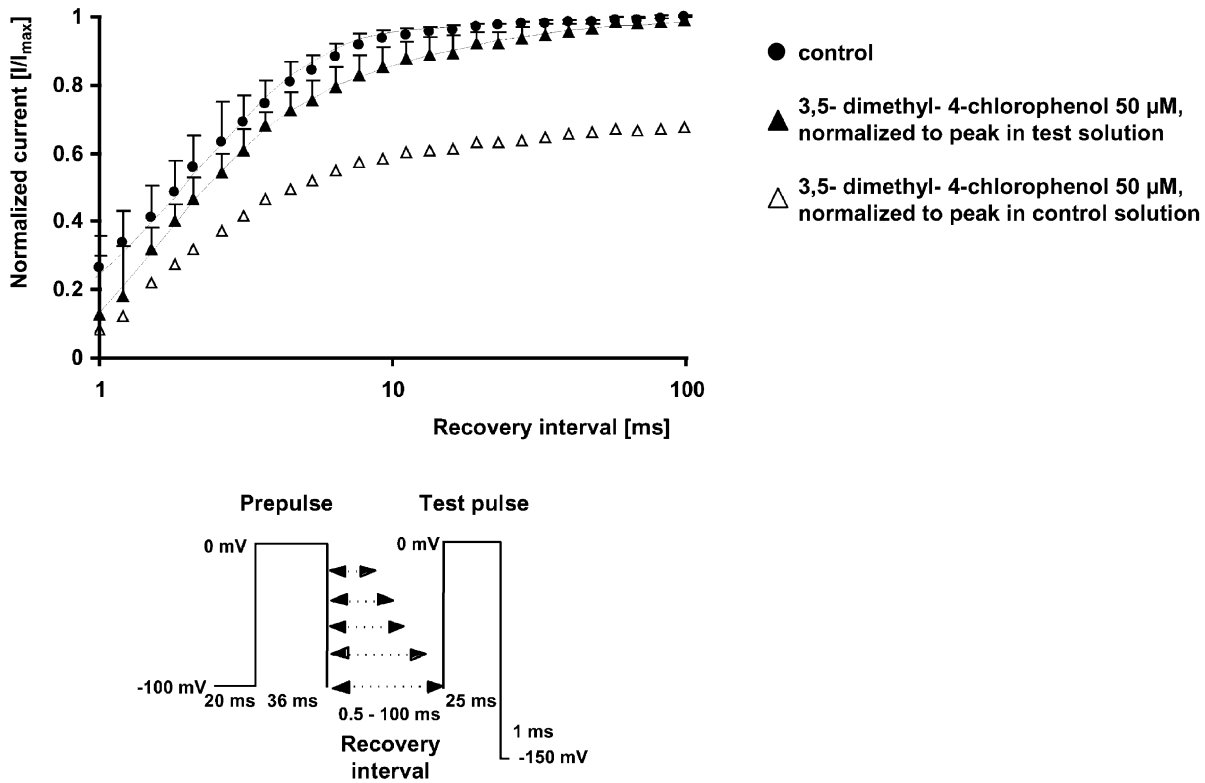

Fig. 4. Recovery from fast inactivation assessed by a two-pulse protocol in control conditions (circles) and in the presence of 50 μM 3,5-dimethyl-4-chlorophenol (squares). The abscissa represents the recovery time interval between inactivating prepulse and test pulse (up to 100 ms) on a logarithmic scale, and the ordinate represents the fractional current (mean ± S.D., $n = 5$) after recovery from fast inactivation. Test pulse currents were normalized either to the prepulse in the presence of drug (filled symbols) or in the controls (empty symbols). Solid lines are exponential fits [$I(t) = a_0 + a_1\exp(-t/\tau_{h1}) + a_2\exp(-t/\tau h_2)$] to the fractional currents. Without drug, the data fitted to a monoexponential. In the presence of drug, recovery was delayed and contained a second slow component, which made up 14% of the current amplitude.

prolonged to 1.9 ± 0.3 ms in 50 μM 3,5-dimethyl-4-chlorophenol, to 2.4 ± 0.6 ms in 100 μM 2-methyl-4-chlorophenol, to 2.0 ± 0.4 ms in 500 μM 4-chlorophenol, and to 1.9 ± 0.2 ms in 1000 μM 3-methylphenol. Fig. 4 shows the time-course of recovery from fast inactivation with and without 50 μM 3,5-dimethyl-4-chlorophenol.

Six experiments were performed to assess possible spontaneous changes in time-dependent recovery from fast inactivation. Starting values derived from biexponential fits to the current having recovered from inactivation were τ_{rec1} 1.78 ± 0.2 ms, τ_{rec2} 99.8 ± 0.1 ms, the amplitude of the second, slow component was 7.6 ± 1.9%. After 3 and 5 min of whole-cell recording, τ_{rec1} was 1.82 ± 0.3 and 1.83 ± 0.2 ms, τ_{rec2} 99.5 ± 0.1 and 99.9 ± 0.1 ms, the amplitude of the slow component was 6.2 ± 2.2% and 5.9 ± 3.2%.

4. Discussion

A wide variety of clinical conditions is characterized by the expression of Na^+ channels with altered inactivation characteristics as a result of hereditary defects, as in Paramyotonia congenita (Lehmann-Horn and Rüdel, 1995), or secondary damage, such as denervation (Marban et al., 1998), hypoxia or ischemia (Ashton et al., 1997; Pu et al., 1998). Thus, it is desirable to find drugs that interfere specifically with on the one hand the altered gating characteristics and with on the other hand membranes that express inactivation-deficient Na^+ channels rather than normal membranes.

Our results show that phenol derivatives exert dual effects on inactivation-deficient mutant channels. On the one hand, all the phenol derivatives that we have studied have lidocaine-like actions, blocking the peak inward current in a concentration-dependent manner. In contrast to lidocaine and mexiletine, which were unable to confer normal kinetics on heterologously expressed mutant sodium channels (Sah et al., 1998), all phenol derivatives uniformly accelerated delayed inactivation kinetics in R1448H. However, high concentrations of the respective compound were required to restore pathologically delayed inactivation to almost wild type values, the time constant of channel inactivation reported for wild type during depolarization to 0 mV being less than 0.8 ms (Chahine et al., 1994a; Wagner et al., 1997). In this concentration range, all compounds equally induced substantial block of the peak current amplitude. However, it should be noted that

all experiments were performed at room temperature (20°C). As gating kinetics in R1448H are highly temperature-sensitive (Chahine et al., 1994b), it is currently difficult to predict the prevailing effect in vivo. In addition, one major result of that study is that acceleration of the current decay was not linked to a certain structural feature of the molecule (for instance, either the chloride or the methyl group, or a combination of both), but paralleled the potency of the respective compound to block the peak current amplitude.

Mutant as well as hypoxically damaged sodium channels may increase sensitivity to a blocking drug by changing the voltage-dependence of channel inactivation (Fan et al., 1996; Pu et al., 1998). We could show that, analogous to lidocaine (Balser et al., 1996; Fan et al., 1996), the estimated affinity of phenol derivatives for the inactivated state was higher than for the resting state. As a consequence, blocking effects of all compounds at a given membrane potential are determined by the apportionment of resting (= low affinity) and fast-inactivated (= high affinity) channels along the voltage axis in the controls. The voltage dependence of inactivation was shifted by about −15 mV in the direction of negative membrane potentials by the mutant R1448H compared to wild type. For comparison, the membrane potential of half-maximum inactivation ($V_{0.5}$) in this study was −69 mV, compared to −51 to −56 mV (Mitrovic et al., 1995; Mitrovic et al., 1994) in wild type. Analogous changes in the voltage-dependence of inactivation have been described for other mutant (Fan et al., 1996) or hypoxically damaged (Pu et al., 1998) sodium channels. Sensitivity to all compounds at −150, −100 and −70 mV holding potential paralleled the voltage-dependence of channel inactivation in R1448H. This implies that any mutant shifting the voltage-dependence of inactivation into the direction of more negative membrane potentials should reveal an increase in sensitivity to the blocking effects of all phenol derivatives at membrane potentials more positive than −100 mV. Efficacy of lidocaine analogues to block channels with altered inactivation properties rather than normally gating Na^+ channels is supposed to rely mainly on the presumed increased sensitivity due to an increased fraction of inactivated channels at physiological holding potentials (Fan et al., 1996; Pu et al., 1998). Our results show that this mechanism can be assumed to hold uniformly for all phenol derivatives as well, as all phenol derivatives that we examined showed an increased affinity for the inactivated state.

Recovery from inactivation has been reported to be accelerated in the mutant compared to wild type (Chahine et al., 1994b; Yang et al., 1994). In this study, $\tau_{rec\ (fast)}$ was 1.8 ms in the mutant compared to 2.8 ms reported for wild type (Wagner et al., 1997). Accelerated recovery from inactivation displayed by the mutant was delayed by all phenol derivatives. Following membrane repolarization, however, recovery from inactivated channel block is faster in the presence of all phenol derivatives compared with lidocaine ($\tau_{rec\ (slow)}$) 30 vs. > 100 ms in case of lidocaine (Fan et al., 1996)), reducing the risk of prolonged channel blockade.

From our results we conclude that phenol derivatives interact with inactivation-deficient Na^+ channels more specifically than the Na^+ channel blockers recommended for therapy of myotonia up to now (Lehmann-Horn and Rüdel, 1995). Besides lidocaine-like actions, all phenol derivatives uniformly tend to correct altered gating characteristics displayed by the mutant, accelerating impaired inactivation kinetics. However, acceleration of impaired inactivation is associated with a strong reduction of sodium channels.

Acknowledgements

We are indebted to Prof. Lehmann-Horn (Ulm) for providing us with transfected cells. We thank Birgitt Nentwig (Dept. of Anaesthesia, Hannover) for taking care of the cell culture, Dr. Hans-Peter Reiffen and Dr. Burkhard Vangerow (Dept. of Anaesthesia, Hannover) for their help with software problems, and Jobst Kilian (Dept. of Neurology, Hannover) for technical support.

References

Ashton, D., Willems, R., Wynants, J., Van Reempts, J., Marrannes, R., Clincke, G., 1997. Altered Na^+-channel function as an in vitro model of the ischemic penumbra: action of lubeluzole and other neuroprotective drugs. Brain Res. 745, 210–221.

Balser, J.R., Bradley Nuss, H., Romashko, D.N., Marban, E., Tomaselli, G.F., 1996. Functional consequences of lidocaine binding to slow-inactivated sodium channels. J. Gen. Physiol. 107, 643–658.

Bean, B.P., Cohen, C.J., Tsien, R.W., 1983. Lidocaine block of cardiac sodium channels. J. Gen. Physiol. 81, 613–642.

Chahine, M., Bennett, P., George, A., Horn, R., 1994a. Functional expression and properties of the human skeletal muscle sodium channel. Pfluegers Arch. 427, 136–142.

Chahine, M., George, A.L., Zhou, M., Ji, S., Sun, W., Barchi, R.L., Horn, R., 1994b. Sodium channel mutations in paramyotonia congenita uncouple inactivation from activation. Neuron 12, 281–294.

Fan, Z., George, A.L., Kyle, J.W., Makielski, J.C., 1996. Two human paramyotonia congenita mutations have opposite effects on lidocaine block of Na^+ channels expressed in a mammalian cell line. J. Physiol. 496, 275–286.

Haeseler, G., Leuwer, M., Kavan, J., Würz, A., Dengler, R., Piepenbrock, S., 1999. Voltage-dependent block of normal and mutant muscle sodium channels by 4-chloro-*m*-cresol. Br. J. Pharmacol. 128, 1259–1267.

Haeseler, G., Petzold, J., Hecker, H., Würz, A., Dengler, R., Piepenbrock, S., Leuwer, M., 2000. Succinylcholine metabolite succinic acid alters steady-state activation in muscle sodium channels. Anesthesiology 92, 1385–1392.

Hamill, O.P., Marty, A., Neher, E., Sakmann, B., Sigworth, F.J., 1981. Improved patch-clamp techniques for high-resolution current recording from cells and cell-free membrane patches. Pfluegers Arch. 391, 85–100.

Hodgkin, A.L., Horowicz, P., 1959. The influence of potassium and

chloride ions on the membrane potential of single muscle fibres. J. Physiol. 148, 127–160.

Hoffman, E.P., Lehmann-Horn, F., Rüdel, R., 1995. Overexcited or inactive: ion channels in muscle disease. Cell 80, 681–686.

Hudson, A.J., Ebers, G.C., Bulman, D.E., 1995. The skeletal muscle sodium and chloride channel diseases. Brain 118, 547–563 (review).

Lehmann-Horn, F., Rüdel, R., 1995. Hereditary nondystrophic myotonias and periodic paralyses. Curr. Opin. Neurol. 8, 402–410.

Marban, E., Yamagishi, T., Tomaselli, G., 1998. Structure and function of voltage-gated sodium channels. J. Physiol. 503, 647–657.

Mitrovic, N., George, A.L., Heine, R., Wagner, S., Pika, U., Hartlaub, U., Zhou, M., Lerche, H., Fahlke, C., Lehmann-Horn, F., 1994. K^+-aggravated myotonia: destabilization of the inactivated state of the human muscle sodium channel by the V1589M mutation. J. Physiol. 478, 395–402.

Mitrovic, N., George, A., Lerche, H., Wagner, S., Fahlke, C., Lehmann-Horn, F., 1995. Different effects on gating of three myotonia-causing mutations in the inactivation gate of the human muscle sodium channel. J. Physiol. 487, 107–114.

Pu, J., Balser, J.R., Boyden, P.A., 1998. Lidocaine action on Na^+ currents in ventricular myocytes from the epicardial border zone of the infarcted heart. Circ. Res. 83, 431–440.

Sah, R.L., Tsushima, R.G., Backx, P.H., 1998. Effects of local anesthetics on Na^+ channels containing the equine hyperkalemic periodic paralysis mutation. Am. J. Physiol. 275, C389–C400.

Wagner, S., Lerche, H., Mitrovic, N., Heine, R., George, A.L., Lehmann-Horn, F., 1997. A novel sodium channel mutation causing a hyperkalemic paralytic and paramyotonic syndrome with variable clinical expressivity. Neurology 49, 1018–1025.

Yang, N., Ji, S., Zhou, M., Ptacek, L.J., Barchi, R.L., Horn, R., George, A.L., 1994. Sodium channel mutations exhibit similar biophysical phenotypes in vitro. Proc. Natl. Acad. Sci. U. S. A. 91, 12785–12789.